AIMS Biophysics, 8(4): 307–317.
DOI: 10.3934/biophy.2021024
Received: 05 July 2021
Accepted: 05 September 2021
Published: 14 September 2021

http://www.aimspress.com/journal/biophysics

Research article

Using elastic scattering to determination of diseases via urine samples

Suleyman Yilmaz*

Aksaray University, Faculty of Education, Department of Sciences, Turkey

*** Correspondence:** Email: yilmazsuleyman@yahoo.com; Tel: +903822883358.

Abstract: In diagnosing the urinary tract and related diseases, the problem of light scattering from human urine was examined on the basis of classical electromagnetic theory. Numerical calculations were made for the designed cylindrical model with the help of optical parameters in the literature obtained from the laboratory test results of urine samples. In the designed model, the changes of the scattered intensity of the light from the urine solution according to the size parameter of the particles and the angular distribution of the system (including forward, side and back scattering) in the equatorial plane were obtained, in both transverse electric (TE) and transverse magnetic (TM) of the polarization states of the light. It was observed that the molecular density changes caused by the materials in the urine sample changed primarily the optical parameters and indirectly the intensity distribution of the scattered light. Thus, with the contribution of standard data provided as a result of light scatter calculations from urine samples taken from people with normal and different diseases, it will be easier to diagnose diseases that will be encountered later.

Keywords: optic parameters; elastic scattering; urinary diseases; clinical diagnosis

1. Introduction

The urinalysis is a laboratory test to help identify problems related to diseases and disorders that occur in lungs, kidneys, urinary tract, bladder and skin are determined from waste and toxic substances in the urine. The urinalysis, which is also used to determine diabetes, kidney, liver disease and urinary tract infections, is needed before surgery, pregnancy examination, routine medical and physical examination. It was known that urinary tract infection is a widespread infectious disease in humans [1]. Urine culture is the standard diagnostic test for determining urinary tract infection in a symptomatic patient and provides information about pathogenic and antibiotic susceptibility [2].

Urinase-producing microorganisms that occur due to stones in the urinary tract cause infection. Bacterial activity, especially from Proteus species, causes these infections [3]. In terms of composition and etiology, the most common type of urinary stone consists of calcium oxalate and is usually caused by treatable metabolic disorders [4]. Bacterial pathogens are mostly transmitted from food, water, animals, hospitals and other clinical settings, and viral infections account for ~70% of all pathogenic diseases in humans. These bacteria are considered harmless until they multiply and accumulate in various parts of the body, which can lead to the development of infection [5]. Bacterial infections are a multidrug-resistant health problem that causes many people to become ill and die. Clinical tests are needed for fast and accurate detection of bacteria in natural or culture-free media [6].

Fast and accurate diagnosis of bacteria, yeast and pathogens for industrial microbiological control and clinical diagnosis requires technology [7]. In classical microbiology, although being inexpensive and allowing both quantitative and qualitative information about the diversity of microorganisms present in a sample, however, these methods are laborious and time consuming (media preparation, dilution, plating, incubation, counting, isolation, and characterization), and results are only observed after several days, and frequently false positives are obtained [8]. With the automation for screening, alternative diagnostic approaches have become mandatory instead of traditional urinalysis. Techniques such as Optical Scattering Technique, Second Harmonic Generation, Consistent Anti-Stokes Raman Scattering, Vibration Spectroscopy, Optical Coherence Tomography, and other spectroscopy and tomography techniques is used to examine changes in cells and tissues [9]. The absence and presence of bacteria, solid phases settled in artificial urine is examined by optical methods, such as X-ray Diffraction, Energy Dispersive X-ray, Scanning Electron Microscopy, as well as Raman and Infrared Spectroscopies [10]. The urine particle analysis lagged far behind hematological screening, as it contains a more complex matrix than blood, due to the large size of urine particles (approximately 1 to 100 μm in diameter) and low concentration [11].

Recent developments have brought improvements to optical design and image analysis to increase classification performances and also to address clinical applications involving non-transparent growth culture media [12]. Flow cytometry screening method is used to speed up positive urine culture estimation by reducing the number of urine cultures. The flow cytometry for bacteria counts are compared to standard urine culture results to evaluate the best cut-off values [13]. Extracellular vesicles are extremely difficult to measure and characterize, and they scatter light very little due to their small size (50 to 200 nm) and a low refractive index. This makes detection by light scattering methods difficult, so most extracellular vesicles cannot be detected by conventional flow cytometry [14]. The vesicles of assorted size, internal contents, and membrane composition are measured by imaging, voltage pulses, and optical spectroscopy [15].

Light scattering is known to be the most useful tool to investigate the structure of particles [16–19]. The light scattering from biological cells depends on the morphological and biochemical structure of the cell. The interaction of light with tissues at the cellular condition potentially encourages the development of optical diagnostic techniques. Structures representing cell organelles such as endoplasmic reticulum tubules, cisterns of the Golgi apparatus, where the visible light is smaller than the wavelength of the light, the light scattering is calculated by Rayleigh scattering. Most subcellular structures produce interesting but complex scattering patterns when smaller than or equal to the wavelength of light. The theory of approximate light scattering by large particles was first proposed in 1957 [20]. The Van de Hulst approximation was originally formulated for spherical particles only. Despite the perfectly spherical shape of inhomogeneous cells and their nuclei,

experimental results were explained using the Mie theory which deals with uniform spheres [21]. Light applications have long been used to monitor tissues and cells to diagnose diseases [22]. The scattering process is determined by the specific wavelength of light, the size of the particle, the angular distribution of the scattered light and its wavelength dependence. Elastic light scattering is widely used to study the size and shape of small particles such as colloids, water droplets and cells. While elastic light scattering is widely used to study the morphology of living tissues, biological tissues cannot be directly measured [23]. So the single scattering component is not the only component of the returned light that can provide valuable diagnostic information and early diagnosis, but while often presented with elastic light scattering, it can even prevent tissues and organelles from succumbing to cancer and save lives [24].

It was the aim of this paper to perform a study of the light scattering by the human urine that is analogous to the structure of biological samples. The vital biological samples, such as blood cells, DNA structures can be effectively detected by light scattering, enabling non-invasive, rapid and automated analysis [25,26]. A sensitive and highly efficient method was used according to the incident electromagnetic field and an analytical procedure was presented to the solutions [27].

2. Urine and urinalysis

Urine is a sterile waste product consisting of water-soluble nitrogen products that are excreted through the urethra from the body. Human urine is yellowish in color and consists of water, urea, creatinine, uric acid and trace amounts of enzymes, carbohydrates, hormones, fatty acids, pigments and inorganic ions such as mucin and sodium. Trace amounts of urobilinogen, urobilin, amino acids, enzymes, purines, nitrogenous hormones and vitamins are included [28].

2.1. Physical properties of urine samples

The physical property of urine consists of color, turbidity, odour, pH and density. Significant changes in physical characteristics may indicate disease or metabolic disorders, even as symptoms of more serious diseases such as diabetes mellitus or a damaged glomerulus. The average pH value of human urine is about 6.2, ranging from 6.2 to 7, with a specific gravity 1.003 to 1.035. Experiments in the clinical laboratory demonstrated acceptable performance of the Abbe refractometer for urine specific gravity, such as handling, sensitivity, accuracy, linearity, analytical sensitivity, and reference range verification. The refractive index values of urine in a human were measured between 1.324 and 1.355 depending on age factor and health status [29]. The dielectric properties and the effect of protein fractions and electrolyte imbalance on the refractive index of serum in multiple myeloma were investigated [30,31]. The urine sample used in the numerical calculation was obtained from the data in the literature, which was collected from people of different age groups between 22 and 60 years of age with random health conditions. The data about the refractive index of urine collected from 25 age groups was presented by using optical glass sensor technique. The average value of refractive index of urine in healthy persons was found to be 1.343, regardless of age [32].

2.2. Chemical elements in human urine

Normal human urine generally consists of water, urea, salts and pigments. The multiplicity of elements in human urine depends on the diet, health and hydration level applied, and human urine consists of some elements such as Oxygen, Nitrogen, Carbon, and Hydrogen. Different substances that cause injury or infection of the glomeruli of the kidneys that can alter the ability of the nephron to re-absorb or filter different components of the blood plasma can be excreted in the urine. For example, diabetes is an endocrine diseases in which the human body has high blood sugar levels because of inability to produce, metabolize or respond to insulin hormone.

3. Numerical solutions of the scattering problem

Analytical and numerical techniques are used to describe light scattering by biological objects such as cell organelles. There are two types of problems with light scattering by a single particle: direct and reverse scattering problems. In the direct problem, when a particle of known structure illuminated by a plane wave with a certain polarization, it is formulated by finding the electromagnetic field inside and outside the particle. In the inverse problem, the distribution of the refractive index of the particle can be found based on the measurable electromagnetic wave scattered by the particle. The opaque, translucent and transparent media are in common use in clinical microbiology. Micro colonies growing in all types of culture media are examined based on the elastic scattering pattern. The forward scattering pattern from opaque materials has been shown to be promising compared to the back scatter pattern [33].

Computer simulations play an important role in the numerical solution of electromagnetic problems in the scattering of light by particles, and in determining the relationship between experiment and theory. There are two numerical methods that have been found to be very useful for studying light scattering from biological objects: the discrete particle model (DPM) [34] and the three-dimensional finite difference time domain (FDTD) method [35].

Computer programs for light scattering are based on standard solutions of Maxwell's equations. In a cylindrical model, light scattering is examined depending on the angle of the intensity of light in the semi-equatorial plane and the size of the particle. In the calculations, the angular dependence of scattered waves is considered as a function of the size parameter, refractive index, the axis of the scattering centers, and polarization plane of the incident waves. In optical elastic scattering, the incident electromagnetic wave interacts with particles of comparable size to the incident wavelength. In this scattering process, although the energy of the incoming electromagnetic wave is conserved, only its direction changes. In this case, the intensity of the scattered electromagnetic wave is proportional to the fourth power of the incoming electromagnetic wave size. This phenomenon is also called Rayleigh scattering in optics and requires the small particle approximation [18,36–38].

Incident, internal and scattered fields were accepted in the same plane and the z-axis was determined as the cylinder axis. The electric fields have only the z component in the case of transverse magnetic (TM) polarization, and the incident, scattered and internal electric fields are as follows:

$$E_Z^{inc}(kr) = E_0 \sum_{n=-\infty}^{\infty} i^n J_n(kr) e^{in\emptyset} \tag{1}$$

$$E_Z^{int}(mkr) = E_0 \sum_{n=-\infty}^{\infty} i^n b_n J_n(mkr) e^{in\emptyset} \tag{2}$$

$$E_Z^{sca}(kr) = -E_0 \sum_{n=-\infty}^{\infty} i^n d_n H_n^{(1)}(kr) e^{in\emptyset} \tag{3}$$

Where, E_0 is the amplitude of the incident electric field and b_n and d_n are unknown internal and scattered field expansion coefficients, respectively. J_n is the Bessel function of the first kind and $H_n^{(1)}$ is the Hankel function of the first kind. m is the complex refractive index of the medium, including the real optical refractive index and the imaginary optical absorption parameter ($m = n - ik$). r is the volumetric radius and $\emptyset$ is the azimuthal angle change in the equatorial plane of the cylindrical scattering center. The other k is the wave vector of the incident, internal and scattered electromagnetic field vectors and determines the size of the scattering centers. At the cylindrical scattering centers, the wave vector depends on the radius size and length of the cylinder. At the boundary conditions, the internal and the scattered field expansion coefficients are

$$b_n = \frac{1}{J_n(mx)}\left[J_n(x) - \left(\frac{mJ_n'(mx)J_n(x) - J_n(mx)J_n'(x)}{mJ_n'(mx)H_n^{(1)}(x) - J_n(mx)H_n'^{(1)}(x)}\right)H_n^{(1)}(x)\right] \quad (4)$$

$$d_n = \frac{mJ_n'(mx)J_n(x) - J_n(mx)J_n'(x)}{mJ_n'(mx)H_n^{(1)}(x) - J_n(mx)H_n'^{(1)}(x)} \quad (5)$$

where, x = ka is the size parameter and prime indicates the derivative with respect to the argument. k is the wave vector of the electromagnetic field.

In transverse electric (TE) polarization, the approach in Eq 1–Eq 3 is used when calculating the magnetic field. Again, the z components of the magnetic field are taken, only the expansion coefficients a_n and c_n instead of b_n and d_n, respectively. Thus, the E_z, E_0 fields in the calculations were also converted to the H_z, H_0 fields.

Other quantities of interest such as the scattered intensity can be written as follows:

$$I(\emptyset, x, m) = \frac{2I_0}{\pi kr}|b_0 + 2\sum_{n=1}^{\infty} b_n Cosn\emptyset|^2 \quad (6)$$

Where, I_0 is the incident intensity, ∅ is the azimuthal angle in the semi equatorial plane. Programs consisting of a main routine and subroutines, using double precision variables, calculated the scattered and internal field expansion coefficients.

4. Numerical results and discussions

In computer calculations, materials representing human urine sample were considered as linear, isotropic and dispersive, that is, the refractive index as a function of wavelength. At the same time, the material was assumed to be an infinite homogeneous, lossless medium and to be isolated in space. Numerical computing programs are based on Maxwell's standard separation of variable solutions. In the small-particle approach, as an alternative solution, for small cylinders the diameter is considered small relative to the wavelength.

Numerical calculations were performed using the scattering properties of homogeneously distributed cylindrical model. The data were obtained with the standard Fortran Power Station 4.0 program and converted into drawings with the help of the Gnuplot graphics program.

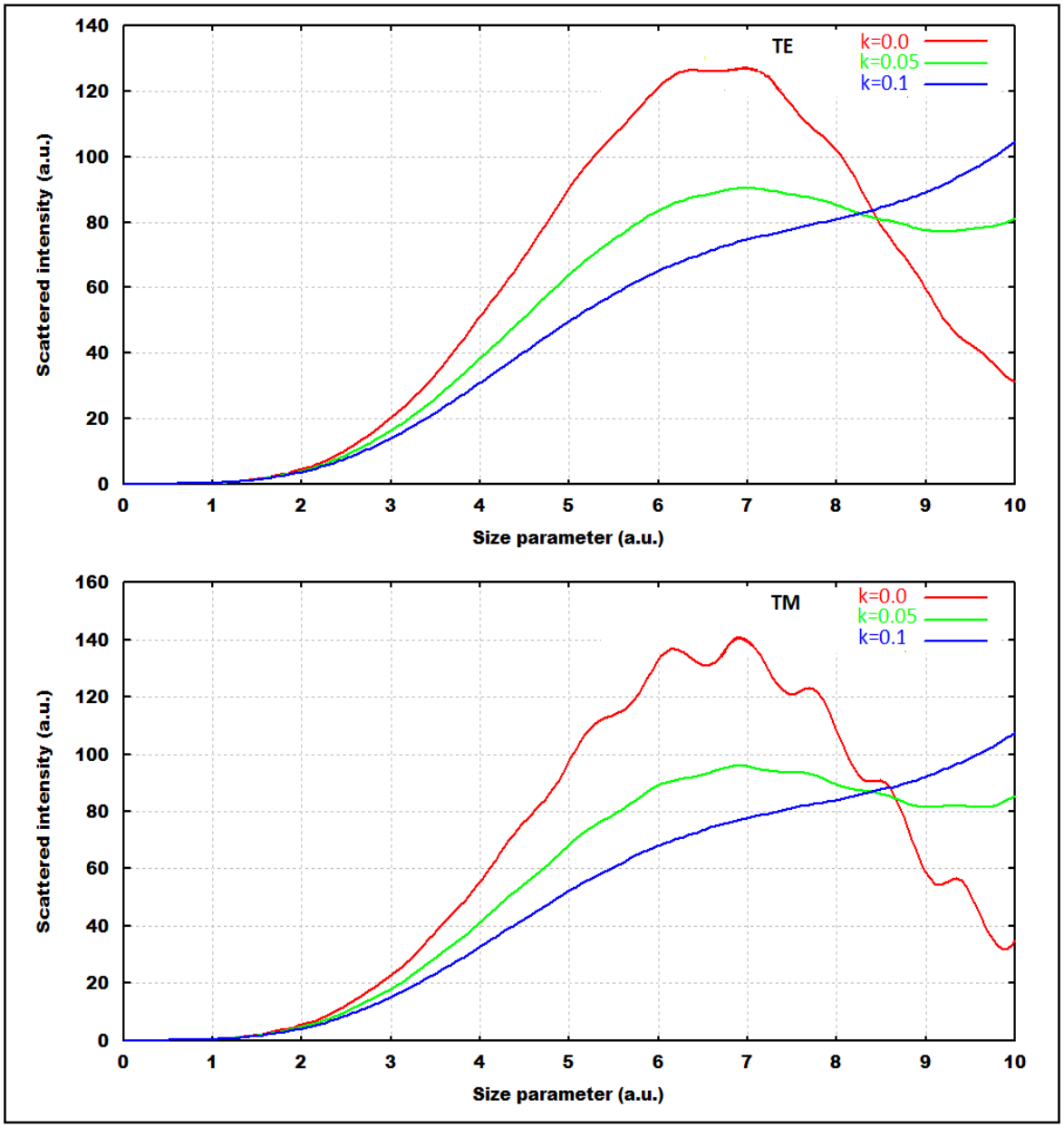

Figure 1. The scattered intensity versus size parameter in TE and TM polarization. The optical absorbance parameters are 0.0, 0.05 and 0.1, respectively.

The variation of the scattered intensity according to the size parameter was given in Figure 1 and to the angular distribution in Figure 2 for both TE and TM polarization cases. In Figures 1 and 2, the scattered intensity versus size parameter curves was seen to be smoother as the absorbency of the sample increasing. The smoothness of the curve is modulated by the absorbency of the sample which characterizes the ingredients of the urine sample. The size parameter was used as an arbitrary unit because of comparable to the dimension of the container of the sample, which was used as the model in the numerical simulation. The model was based on the size of the cylindrical capillary tubes when calculating the light scattering from each urine samples. In numerical calculations, the wavelength of the incident light was determined to be comparable in size according to the size parameter. The size parameter for the specified cylindrical geometry was taken as 10 units in the arbitrary unit. The

optical absorbance parameter of each urine sample, for no particular reason, was set at a regular increase of 0.0, 0.05 and 0.1, respectively. In the examined urine samples, the comparison was made according to the scattering centers represented by the molecular representing different disease variations, but by associating them with the variation of the molecular density of the urine sample. It is known that insulin resistance in the liver and hypoglycemia or infection in the urinary tract change the concentration of particles in the urine samples. HeNe laser with a wavelength of 632.8 nm was taken as the wavelength source of the incident electromagnetic wave.

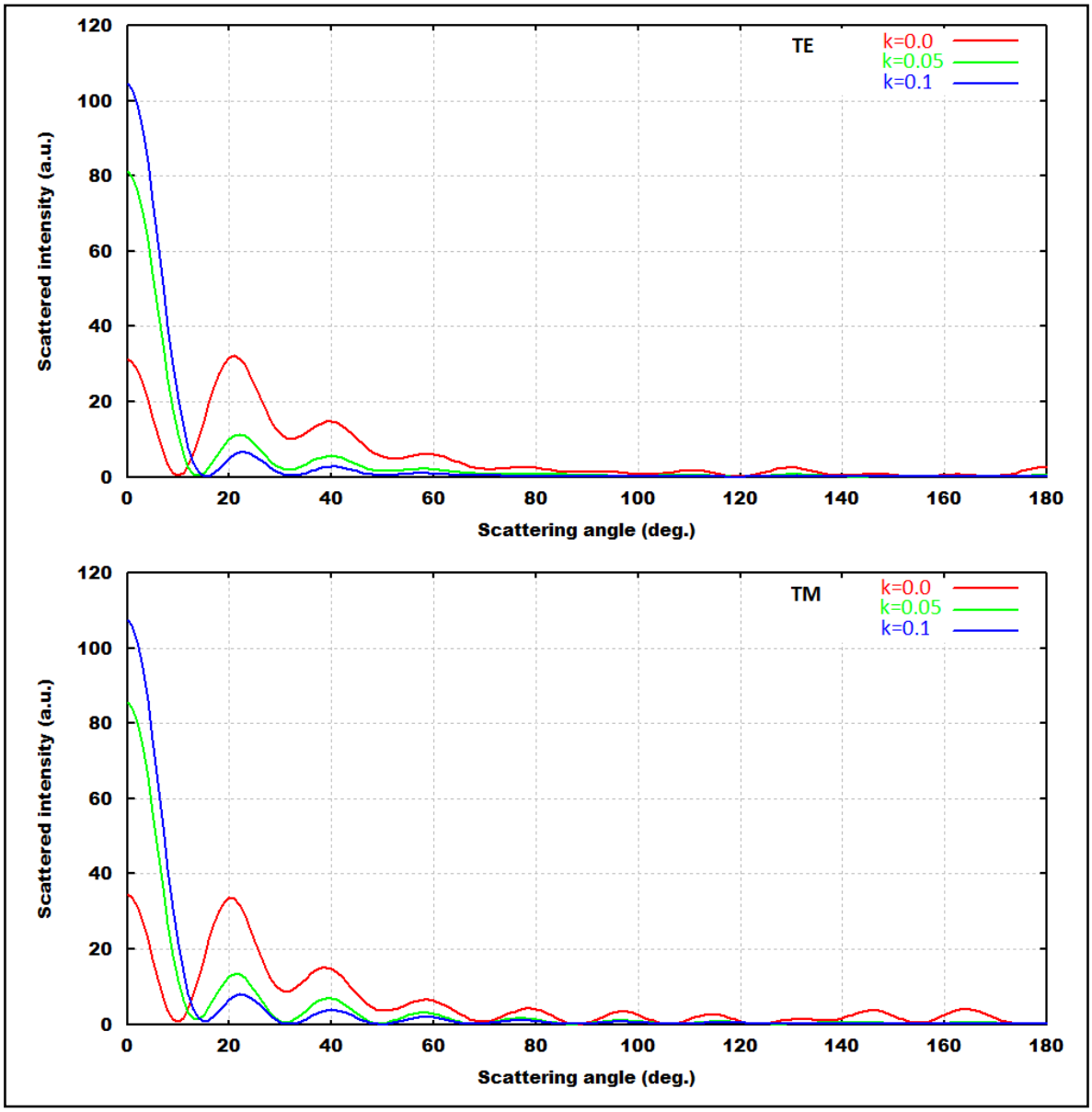

Figure 2. The scattered intensity versus azimuthal angle in TE and TM polarization. The optical absorbance parameters are 0.0, 0.05 and 0.1, respectively.

The maximum intensities versus the size parameters of the urine samples were obtained as 127.025, 90.437 and 74.957 for TE polarization, 140.888, 96.017 and 77.994 for TM polarization in cases of non-adsorbing, absorbing, and more absorbing medium, respectively.

As the absorbance of the molecular environment increases, the scattered intensity values change dramatically to low levels in two polarization cases in Figure 1.

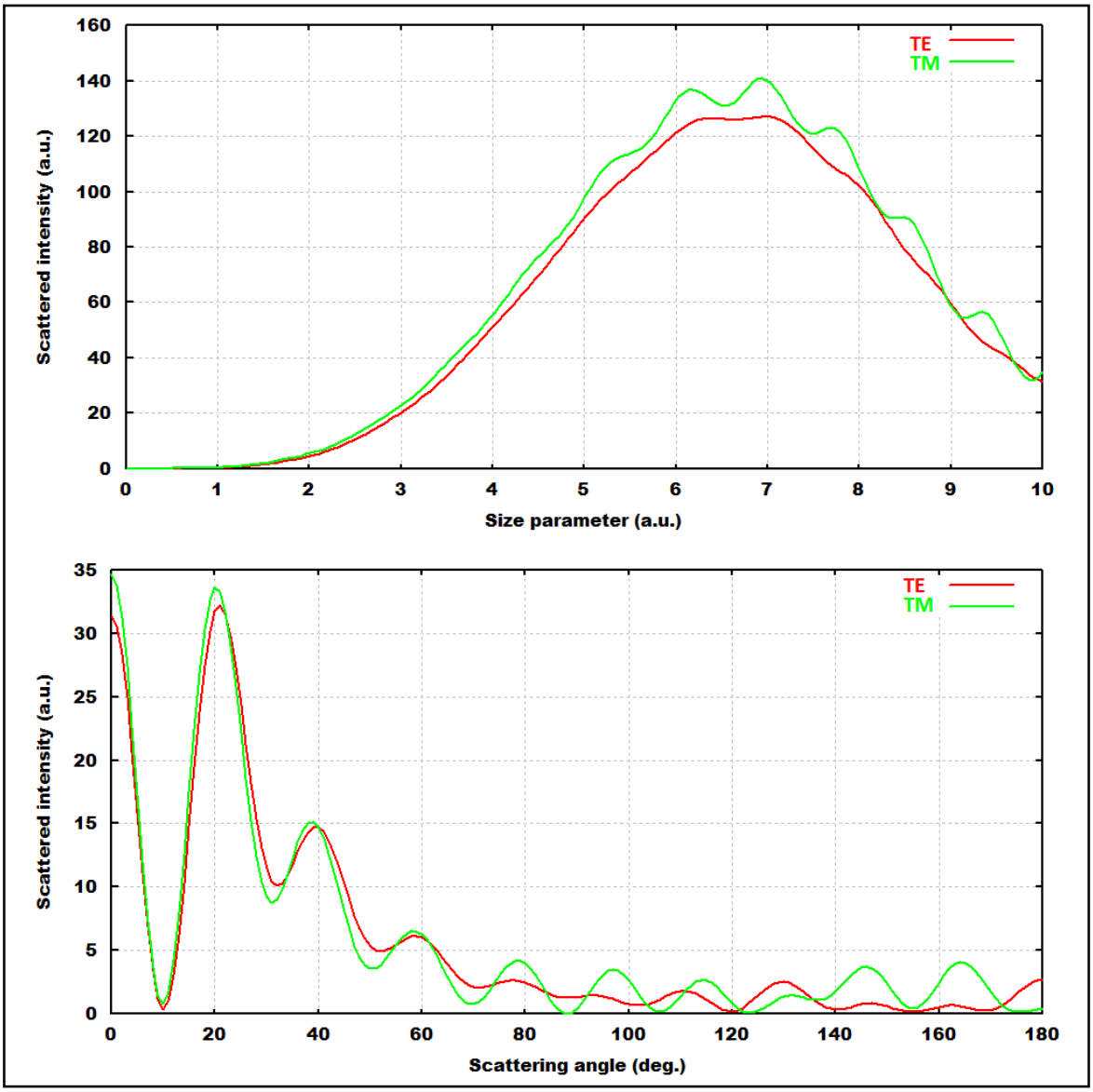

Figure 3. Comparison of the scattered intensity within each TE and TM polarization cases. The scattering angle in the top figure is 0.0 degree and the size parameter in the bottom figure is 10 in arbitrary units. The optical absorbance parameter is 0.0.

The scattered intensities versus the azimuthal angle in the equatorial plane of the urine samples were obtained as 31.334, 81.216 and 104.605 for TE polarization, 34.653, 85.568 and 107.517 for TM polarization in cases of non-absorbing, absorbing, and more absorbing medium, respectively. In the equatorial plane, the angular distribution of the intensity of scattered light exhibits an exponential decrease for forward, side and backward scattering for two polarization cases in Figure 2. TE and TM polarization cases were compared with the change of scattered light according to the size parameter and scattering angle under non-absorbing conditions in Figure 3.

In the change of scattered intensity according to the size parameter, the level of scattered

intensity in TM polarization is higher than in TE polarization. On the other hand, the change of scattered intensity with respect to azimuthal angle, the level of scattered intensity in TM polarization is lower than in TE polarization.

5. Conclusions

Numerical calculations have shown that the optical light scattering method gives important results in the molecular change of the urine sample. The scattered intensity increases gradually while the particle size increases in both TE and TM polarization cases in Figure 1. The molecular density change in the urine sample representing the disease state changes the absorbance of the medium, so that the intensity distribution of the scattered light increases by oscillating at low molecular density, while achieving a flat increase in high molecular density. The intensity of the scattered light drastically decreases with the angular change in the semi-equatorial plane for TE and TM polarization, in Figure 2. As the absorbance of the urine sample increases, it is observed that the curves of the scattered light are damped more sharply. In the analysis of urine by optical method, standard density distributions are obtained primarily depending on the change of chemical samples in the urine. The standards obtained provide valuable information about the urine sample whose density distributions are to be examined later and whose contents are unknown.

In the change of scattered intensity according to the size parameter, the level of scattered intensity in the TM polarization is higher than that of the TE polarization because the oscillation plane of the incoming wave is different in Figure 3. With a similar approach, the change of scattered intensity relative to the azimuthal angle appears to be lower than the diffused density level TE polarization in TM polarization.

This study, which is presented by using the refractive index of human urine, provides useful information and important data for the diagnosis of a disease that develops in the human body. With the help of the refractive index of urine, which concerns the molecular density change, the diagnosis of a disease can contribute to knowing the effect of the drug, monitoring and curing the disease. Standards established by refractive index data of urine obtained from patients who have already been exposed to various diseases can be a complementary parameter for evaluating new degrees of disease and its nature in the medical discipline. The optical technique based on the elastic scattering method can serve as a potential tool for assessing a patient's physiological and ecological conditions as well as body chemistry. We can easily say that the analysis that can be done with optical methods is a very fast, accurate and simple method for analyzing biological fluids such as serum, plasma, spinal fluid and urine.

In summary, the elastic light scattering technique can be used to early detect and diagnose lesions of diseases in vivo in the urine sample. Therefore, it reduces the cost and increases the effectiveness of traditional diagnostic methods. The results obtained from the scattering properties of urine samples in the designed model are consistent with other studies in the literature and our current studies on biological samples. [25–27,36,37,39]. This study will encourage how the refractive indices of urine samples representing various diseases can be deciphered and how the disease can be diagnosed for further studies based on the density distribution.

Conflict of interest

The author declares no conflict of interest. No funding has been received from anywhere for this

study. Also, ethical approval is not required.

References

1. Foxman B (2014) Urinary tract infection syndromes: occurrence, recurrence, bacteriology, risk factors, and disease burden. *Infec Dis Clin N Am* 28: 1–13.
2. Medina-Bombardó D, Jover-Palmer A (2011) Does clinical examination aid in the diagnosis of urinary tract infections in women? A systematic review and meta-analysis. *BMC Fam Pract* 12: 111.
3. Benramdane L, Bouatia M, Idrissi MOB, et al. (2008) Infrared analysis of urinary stones, using a single reflection accessory and a KBr pellet transmission. *Spect Lett* 41: 72–80.
4. Petrova EV, Gvozdev NV, Rashkovich LN (2004) Growth and dissolution of calcium oxalate monohydrate (COM) crystals. *J Optoelectron Adv Mater* 6: 261–268.
5. Smith KF, Goldberg M, Rosenthal S, et al. (2014) Global rise in human infectious disease outbreaks. *J R Soc Interface* 11: 0950.
6. Locke A, Fitzgerald S, Mahadevan-Jansen A (2020) Advances in optical detection of human-associated pathogenic bacteria. *Molecules* 25: 5256.
7. Newell DG, Koopmans M, Verhoef L, et al. (2010) Food-borne diseases—the challenges of 20 years ago still persist while new ones continue to emerge. *Int J Food Microbiol* 139: 3–15.
8. Bhunia AK (2014) One day to one hour: How quickly can foodborne pathogens be detected? *Future Microbiol* 9: 935–946.
9. Tuchin V (2015) Tissue optics: light scattering methods and instruments for medical diagnostics, 3 Eds., Bellingham: SPIE Press.
10. Prywer J, Kozanecki M, Mielniczek-Brzóska E, et al. (2018) Solid phases precipitating in artificial urine in the absence and presence of bacteria. *Crystal* 8: 164.
11. Delanghe JR (2007) New screening diagnostic techniques in urinalysis. *Acta Clin Belg* 62: 155–161.
12. Genuer V, Gal O, Méteau J, et al. (2016) Optical elastic scattering for early label-free identification of clinical pathogens, advanced biomedical and clinical diagnostic and surgical guidance systems. *International Society for Optics and Photonics*.
13. Moshaver B, de Boer F, van Egmond-Kreileman H, et al. (2016) Fast and accurate prediction of positive and negative urine cultures by flow cytometry. *BMC Infect Dis* 16: 21.
14. Gardiner C, Shaw M, Hole P, et al. (2014) Measurement of refractive index by nanoparticle tracking analysis reveals heterogeneity in extracellular vesicles. *J Extra Vesic* 3: 25361.
15. Buzás EI, Gardiner C, Lee C, et al. (2016) Single particle analysis: Methods for detection of platelet extracellular vesicles in suspension (excluding flow cytometry). *Platelets* 28: 249–255.
16. Barber PW, Hill SC (1990) Light scattering by particles: computational methods. *World Scientific*, Singapore: 276.
17. Sheng P (1995) Introduction to wave scattering, localization, and mesoscopic phenomena. *San Diego*: Academic Press, 45–74.
18. Bohren CF, Huffman DR (1983) Absorption and scattering of the light by small articles. *John Wiley & Sons, New York*.
19. Barber PW, Huffman DR (1990) Light scattering by small particles computational methods. *World Scientific*, Singapore: 25–77.
20. van de Hulst HC (1957) Light scattering by small particles. *Phys Today* 10: 28.

21. Hammer M, Schweitzer D, Michel B, et al. (1998) Single scattering by red blood cells. *Appl Opt* 37: 7410–7418.
22. Chance B (1991) Optical method. *Annu Rev Biophys Biophys Chem* 20: 1–28.
23. Yodh AG, Chance B (1995) Spectroscopy and imaging with diffusing light. *Phys Today* 48: 34–40.
24. Backman V (1998) Early diagnosis of cancer using light scattering spectroscopy. *Mass Inst Technol.*
25. Yilmaz S, Kalkandelen A, Mamedova NI (2006) Comparison of the T-matrix calculations for erythrocytes with oxygenated hemoglobin and immersed in water. *J Quant Spectrosc Radiat Transfer* 97: 20–28.
26. Yilmaz S, Koc H (2005) Light scattering by DNA structure due to phase transition. *Mol Phys* 103: 2633–2637.
27. Mishchenko MI, Travis LD, Macke A (1996) Scattering of light by polydisperse, randomly oriented, finite circular cylinders. *Appl Opt* 35: 4927–4940.
28. Plummer DT, Leathwood PD (1967) Some properties of lactate dehydrogenase found in human urine. *J Biochem* 103: 172–176.
29. Wyness-Sara P, Hunsaker-Joshua JH, Snow-Taylor M, et al. (2016) Evaluation and analytical validation of a handheld digital refractometer for urine specific gravity measurement. *Pract Lab Med* 5: 65–74.
30. Lonappan A, Hamsakkutty V, Bindu G, et al. (2004) Dielectric properties of human urine at microwave frequencies. *Microw Opt Techn Lett* 42: 500–503.
31. Plotnikova L, Polyanichko A, Kobeleva M, et al. (2017) The Influence of protein fractions and electrolyte imbalance on refractive index of serum in patenti with multiple myeloma. *J phys conf ser* 784: 012047.
32. Rao SV (2010) Study of multimode fiber optic sensor. PhD thesis of Jawaharlal Nehru Technological University.
33. Guo S (2004) Optical scattering for bacterial colony detection and characterization. *Purdue University*.
34. Schmitt JM, Kumar G (1998) Optical scattering properties of soft tissue: a discrete particle model. *Appl Opt* 37: 2788–2797.
35. Dunn A, Kortum-Richards R (1996) Three-dimensional computation of light scattering from cells. *IEEE J Sel Top Quantum Electron* 2: 898–905.
36. Travis LD, Mishchenco MI (1994) Light scattering by polydispersions of randomly oriented spheroids with sizes comparable to wavelengths of observation. *App Opt* 33: 7206.
37. Videen G, Ngo D (1997) Light scattering from a cylinder near a plane interface: theory and comparison with experimental data. *J Opt Soc Am A* 14: 70.
38. van de Hulst HC (1981) Light scattering by small particles. New York: Dover Publications, Inc.
39. Yilmaz S (2012) Determination of the structural properties of a columnar hexagonal liquid crystal by light scattering. *J Mod Opt* 59: 912–916.

AIMS Press